J. Korean Soc. Ind. Appl. Math. Vol.23, No.4, 351–365, 2019 http://doi.org/10.12941/jksiam.2019.23.351

AN OPTIMAL CONTROL APPROACH TO CONFORMAL FLATTENING OF TRIANGULATED SURFACES

YESOM PARK[1], BYUNGJOON LEE[2], AND CHOHONG MIN[1†]

[1]DEPARTMENT OF MATHEMATICS, EWHA WOMANS UNIVERSITY, SOUTH KOREA

[2]DEPARTMENT OF MATHEMATICS, THE CATHOLIC UNIVERSITY OF KOREA, SOUTH KOREA
Email address: chohong@ewha.ac.kr

ABSTRACT. This article presents a new approach for conformal flattening with optimal cone singularity. The algorithm here takes an optimal control for selecting optimal cones and uses the Ricci flow to force the flattening. This work is considered as a modification to the work of Soliman et al. [1] in the sense that they make use of the Yamabe equation for the flattening, which is an approximation of the Ricci flow. We present a numerical algorithm based on the optimal control with the mathematical background. Several numerical results validate that our method is optimal in total cone angle and usage of the Ricci flow ensures the conformal flattening while selecting optimal cones.

1. INTRODUCTION

Conformal flattening has been successfully utilized to find a conformal mapping from a surface in $\mathbb{R}^3$ to a region in $\mathbb{R}^2$. The map enables to seamlessly wrap up the surface by a texture image on the region. The texture mapping has been a very important tool in computer graphics [2, 3] and brain mapping [4]. Conformal flattening has been thoroughly studied in mathematics [5] and computer graphics [6]. Being conformal, the map preserves each local angle, but length scale can vary by a large amount.

Researchers such as [7] and [8] suggested a methodology to reduce the length distortion based on Ricci flow, a way to implement conformal flattening .The Ricci flow [9] on a surface leads to the heat flow on its Gaussian curvatures and follows the uniformization of the curvatures to their average value. When a surface is of genus one, the average is zero by the Gauss-Bonnet theorem, and the uniformization results in conformal flattening. Their idea is to allow non-zero curvature at some critical vertices such as the vertices with the largest length distortion. The surface that is flat everywhere except at the singular vertices locally forms a shape of cone at each singular vertex. This is the reason why the methodology is referred to as cone singularity.

Received by the editors September 10 2019; Accepted December 4 2019; Published online December 25 2019.
2000 *Mathematics Subject Classification.* 34H05, 49J15,53C44.
Key words and phrases. Conformal Flattening, Cone Singularity, Discrete Ricci Flow, Optimal Control.
† Corresponding author.

The main issues in practice of the methodology are in selecting the singular vertices and determining their cone angles. Springborn et al. in [10] proposed an explicit and direct approach. They first solve Ricci flow and select the vertices of extreme length distortion as the singular ones, and then resolve Ricci flow with natural boundary condition on the singular vertices to determine the cone angles. This process is repeated to increase the number of cones and decrease the total distortion under a desired amount. The sequential process is an ad hoc approach and poses a question about its optimality, for it was notices that the total distiotion could be further reduces [8] .

Soliman et al. [1] proposed a more systematic approach for the optimal placement of cone singularities. They notices that the cone singularites can be represented by a linear summation of delta functions, and utilized the L^1 minimization approach in image denoizing [11] and compressive sensing [12, 13]. Furthermore, they could significantly reduce the total distortion and decrease the support of cone singularities by solving the dual optimization, instead of the L^1 minimization. Ricci flow is a nonlinear differential equation, and it may take quite a time to obtain its stationary solution. To the contrary, Yamabe equation is a linear equation and its solution is just given by solving the linear equation. Yamabe equation is an efficient means to approximate the stationary solution of Ricci flow. From these reasons, Soliman et al. [1] solved their optimization problem based on Yamabe equation, not based on Ricci flow.

In this work, we point out that the error of Yamabe approximation can be quite large and the measure of total distortion based on the approximation can be misleading. Instead of the optimization based on Yamabe equation, we introduce a novel optimization based on the Ricci flow, equipped with the optimal control. After this introduction, Ricci flow and Yamabe equation are reviewed and compared in section 2. Section 3 give a brief review of the cone singularity. The optimal control problem and a numerical method for solving the problem are introduced in section 4. Numerical results validating our optimizations are presented in section 5, and follows the conclusion of this work and some remarks in section 6.

2. CONFORMAL FLATTENING

In this section, we review the discrete Ricci flow [14], a standard method for conformal flattening of triangulated surfaces. Also we review the discrete Yamabe equation in [1], and show that it is an approximation to obtain the stationary solution to Ricci flow. Compared to Ricci flow that is nonlinear and requires quite a time to have its stationary solution, Yamabe equation is linear and produces its solution by solving a single linear system. Being a simple approximation, Yamabe equation fails to achieve the conformal flattening exactly, while Ricci flow succeeds to do.

Assume a triangulated surface Ω that is given with its vertex set V, edge set E, and face set F. The length of an edge $e_{ij} \in E$ is denoted by l_{ij}, and the angle of a face $\triangle_{ijk} \in F$ opposite to edge e_{jk} by θ^i_{jk}. The flatness of the surface is measured by discrete Gaussian curvature $K : V \to \mathbb{R}^{|V|}$. The discrete Gaussian curvature K_i at a vertex $v_i \in V$ is defined as

$$K_i = 2\pi - \sum_{\triangle_{ijk} \in F} \theta^i_{jk}.$$

For a conformal factor $u : V \to \mathbb{R}^{|V|}$, each length is modified as $l_{ij} = l^0_{ij} \exp\left(\frac{1}{2}u_i + \frac{1}{2}u_j\right)$, where l^0_{ij} is the initial length of the surface. Ricci flow seeks a conformal factor to eliminate all the Gaussian curvatures. A change on conformal factor sequentially leads to the changes of lengths, angles, and curvatures. The sequential dependence of curvature to conformal factor is described by the following lemma. Its proof is a mere implicit differentiation of the cosine law, so we omit the details.

Lemma 2.1. *Assume a vertex function $u(t) : V \to \mathbb{R}^{|\mathbb{V}|}$ that is differentiable with respect to t, then the discrete Gaussian curvature $K(t) : V \to \mathbb{R}^{|\mathbb{V}|}$ is also differentiable and satisfies*

$$K'(t) = -\Delta_{u(t)} u'(t).$$

In the lemma, Δ_u denotes the discrete Laplace-Beltrami operator. For a function $f : V \to \mathbb{R}^{|V|}$, its Laplacian $\Delta_u f : V \to \mathbb{R}^{|V|}$ is defined as

$$(\Delta_u f)_i \quad = \quad \frac{1}{2} \sum_{\triangle_{ijk} \in F} \left[\cot \theta^j_{ki} \left(f_k - f_i \right) + \cot \theta^k_{ij} \left(f_j - f_i \right) \right]$$

Here each $\theta^i_{jk} = \theta^i_{jk}(u)$ is the induced angle by the conformal factor u. Ricci flow evolves the conformal factor $u(t)$ as follows.

$$u'(t) = -K(u(t)) \tag{2.1}$$

Using lemma 2.1, we can prove the conformal flattening of Ricci flow.

Theorem 2.1. *(Conformal flattening) Assume a closed triangulated surface with genus one, so that $|V| - |E| + |F| = 0$. For the Ricci flow, we have $\lim_{t\to\infty} K_i(t) = 0$ for each $v_i \in V$.*

Proof. Being simple and short, we provide a proof though it is well known.

$$\begin{aligned}
\frac{d}{dt}\left[\sum_{v_i \in V} \frac{1}{2} K_i(t)^2\right] &= \sum_{v_i \in V} K_i(t) \cdot K_i'(t) \\
&= -\sum_{v_i \in V} K_i(t) \cdot \left(\Delta_{u(t)} u'(t)\right)_i \\
&= \sum_{v_i \in V} K_i(t) \cdot \left(\Delta_{u(t)} K(t)\right)_i \\
&\leq 0
\end{aligned}$$

The Laplacian is known to be negative definite on subspace $1^\perp$, and the L^2 norm should decrease until $K(t) \in span(1)$. Due to the discrete Gauss-Bonnet theorem [5], the sum

$\sum_{v_i \in V} K_i(t) = 2\pi \cdot (|V| - |E| + |F|) = 0$, for any time t. Thus as time goes on, $\lim_{t\to\infty} K(t) \in span(1) \cap 1^{\perp} = \{0\}$. □

The above theorem shows the convergence of curvature $K(t)$, but the convergence of the vertex function $u(t)$ is not in its scope. The convergence of $u(t)$ can be explained by the convex energy functional $E(u)$ utilizing the Lobachevsky function $\Lambda(x) = -\int_0^x \log|2\sin t|\, dt$ [10]. The functional is defined as

$$E(u) = \sum_{t_{ijk} \in T} \left(\theta_{jk}^{i} \lambda_{jk} + \theta_{ki}^{j} \lambda_{ki} + \theta_{ij}^{k} \lambda_{ij} - \pi (u_i + u_j + u_k) \right) + 2\pi \sum_{v_i \in V} u_i + 2 \sum_{t_{ijk} \in T} \left(\Lambda\left(\theta_{jk}^{i}\right) + \Lambda\left(\theta_{ki}^{j}\right) + \Lambda\left(\theta_{ij}^{k}\right) \right), \tag{2.2}$$

where $\lambda_{ij} = 2 \log l_{ij}$ for each $e_{ij} \in E$. The following theorem shows the convergence of $u(t)$. Its proof can be found in [10].

Theorem 2.2. *(Convergence of $u(t)$) the functional $E(u)$ is convex and strictly convex on $u \in 1^{\perp}$, and has a unique global minimum u^*. The discrete Ricci flow is just the gradient-descent dynamics of the functional. Therefore* $\lim_{t\to\infty} u(t) = u^*$.

For the stationary solution u^*, its induced Gaussian curvature K^* is zero by the conformal flattening. Consider an ansatz $u(t) = tu^*$, $t \in [0, 1]$. According to lemma 1, we get $K'(0) = \Delta_{u(0)} u^*$. Using an approximation $K'(0) \simeq K(1) - K(0) = 0 - K(0)$, we have

$$-\Delta_{u(0)} u^* \simeq K(0).$$

Yamabe equation is the following linear elliptic equation.

$$-\Delta_{u(0)} u^{Yamabe} = K(0).$$

Comparing the above two equations, we observe that u^{Yamabe} is an approximation of u^*. Figure 1 shows that the Gaussian curvature induced by u^{Yamabe} may not be zero by a large margin, while that by u^* is zero within error bound 10^{-5}. The triangulated surface modulated with u^* can be seamlessly embedded on a plane to fit in a rectangle with periodic boundary conditions. However, the error of u^{Yamabe} hinders such seamless fitting.

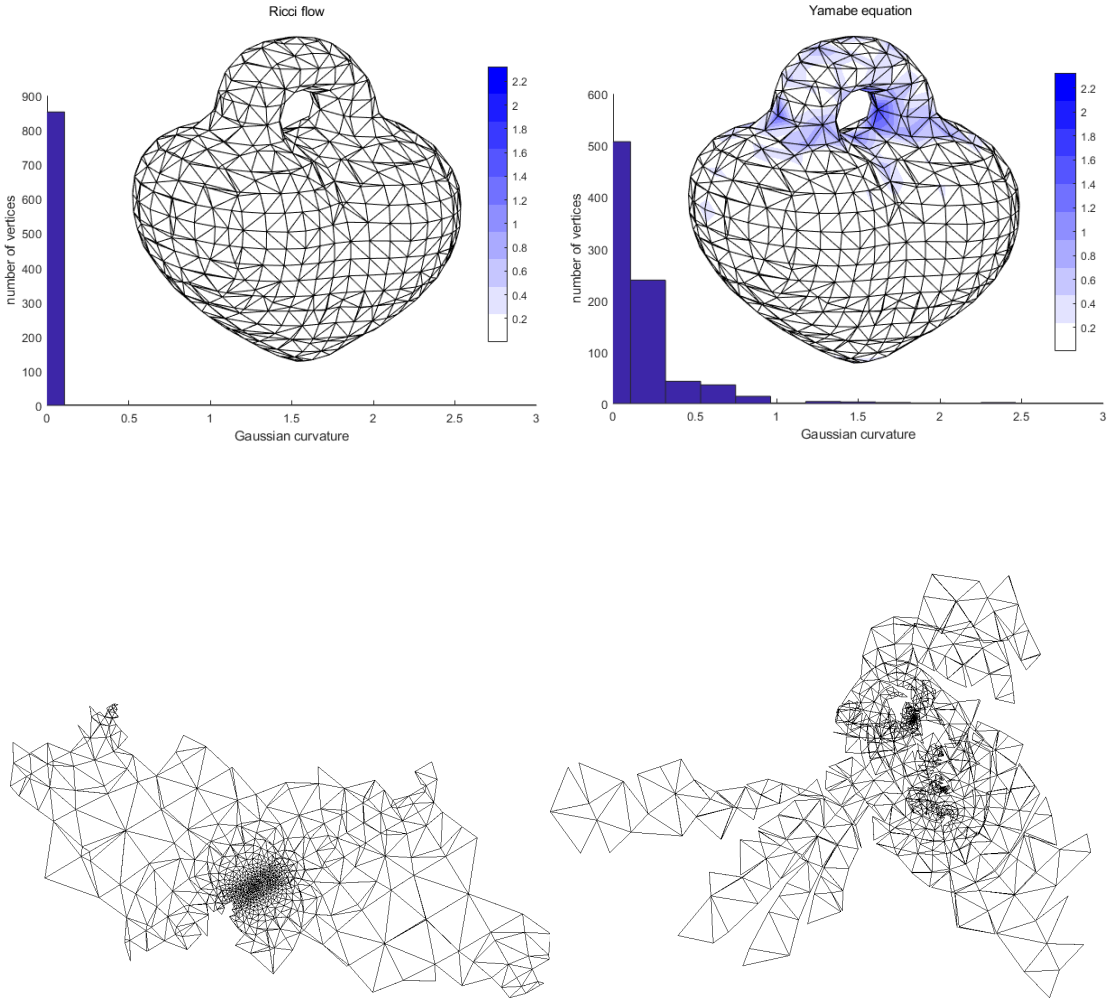

FIGURE 1. Distributions of the Gaussian curvature K^* induced by the Ricci flow (top left) and K^{Yamabe} by the Yamabe equation (top right). Flattening surface modulated with u^* (bottom left) and the surface with u^{Yamabe} (bottom right).

3. CONE SINGULARITY

Conformal flattening may undergo severe length distortion, while it keeps conformality, the cross ratios. The method of cone singularity is to allow non-zero curvature at some vertices in order to reduce the length distortion. Surface at the vertices locally forms a cone shape. That is why it is called cone singularity. The issues in practice are where to put the singularities and how much to choose the angle of each cone. The greedy method suggested by Springborn et

al. [10](**CETM**) iteratively conformally flattens the mesh and inserts a new cone at the vertex with the largest $|u_i|$. In each iteration, instead of prescribing cone angles, they set $u_i = 0$ at cone vertices and cone angles are automatically determined by the flattening process. Soliman et al. [1](**MAD**) proposed the following L^1 minimization problem to resolve the issues.

$$\begin{aligned} &\underset{f\in L^1(\Omega)}{\text{minimize}} \ \frac{1}{2}\left\|u^{Yamabe}\right\|_{L^2}^2 + \lambda \|f\|_{L^1} \\ &\text{subject to } \ -\Delta_{u(0)}u^{Yamabe} = K(0) - f \ \text{in}\,\Omega \end{aligned}$$

The L^1 minimization would have a sparse solution $f = \sum_i \theta_i \delta_{P_i}$, which leads to taking cone singularities at v_i with angle θ_i. As presented in the previous section, Ricci flow solution u^* is superior to u^{Yamabe} in conformal flattening. Thus we consider the following control problem.

$$\underset{f\in L^1(\Omega)}{\text{minimize}} \ C[f] := \frac{1}{2}\|u^*\|_{L^2}^2 + \lambda \|f\|_{L^1} \tag{3.1}$$

$$\text{subject to } u'(t) = -K(u(t)) + f \text{ and } u^* = \lim_{t\to\infty} u(t) \ \text{in}\,\Omega \tag{3.2}$$

4. Conformal flattening based on the optimal control

Our main goal is to solve the optimal control problem (3.1) with Ricci flow dynamics (3.2). In this section, we propose a numerical method for solving the problem with computational details.

4.1. **Discrete setting of Optimal Control.** First, apply the forward Euler method to the singular Ricci flow (3.2)

$$\begin{cases} \frac{u_i^{n+1}-u_i^n}{\triangle t^n} & = -K_i(u^n) + f_i, \ n = 0, \dots N-1 \\ u_i^0 & = 0. \end{cases}, \ \forall v_i \in V \tag{4.1}$$

Then the terminal time is set to be

$$T = \sum_{n=0}^{N-1} \triangle t^n.$$

When we consider the perturbation of the cone singularity $f + \epsilon g$, (4.1) is modified as follows:

$$\begin{cases} \frac{(u_\epsilon)_i^{n+1}-(u_\epsilon)_i^n}{\triangle t^n} & = -K_i(u_\epsilon^n) + f_i + \epsilon g_i, \ n = 0, \dots N-1 \\ (u_\epsilon)_i^0 & = 0. \end{cases}, \ \forall v_i \in V$$

Then, the directional derivative $z(t) := \nabla u[f]\cdot g$ satisfies the following approximated equation

$$\begin{cases} \frac{z_i^{n+1}-z_i^n}{\triangle t^n} & = \triangle_{(u^n)} z_i^n + g_i, \ n = 0, \dots N-1 \\ z_i^0 & = 0. \end{cases}, \ \forall v_i \in V$$

$$\iff z^{n+1} = \left(I + \triangle t^n \triangle_{(u^n)}\right) z^n + \triangle t^n g. \tag{4.2}$$

The cost function is discretized as

$$C_\delta[f] = \lambda \sum_{i \in V} \sqrt{f_i^2 + \delta} + \frac{1}{2} \sum_{i \in V} \left(u_i^N\right)^2.$$

Let us introduce the costate variable p which satisfies the terminal condition

$$p^N = u^N.$$

Using (4.2), we can deduce that

$$\begin{aligned}
&\frac{d}{d\epsilon} C_\delta[f + \epsilon g] \mid_{\epsilon=0} \\
&= \left\langle u^N, z^N \right\rangle + \lambda \left\langle \frac{f}{\sqrt{f^2 + \delta}}, g \right\rangle \\
&= \left\langle p^N, z^N \right\rangle - \left\langle p^0, z^0 \right\rangle + \lambda \left\langle \frac{f}{\sqrt{f^2 + \delta}}, g \right\rangle \\
&= \sum_{n=0}^{N-1} \left[\left\langle p^{n+1}, z^{n+1} \right\rangle - \left\langle p^n, z^n \right\rangle \right] + \lambda \left\langle \frac{f}{\sqrt{f^2 + \delta}}, g \right\rangle \\
&= \sum_{n=0}^{N-1} \left[\sum_{i \in V} \left\langle p^{n+1}, \left(I + \triangle t^n \triangle_{(u^n)}\right) z^n + \triangle t^n g \right\rangle - \left\langle p^n, z^n \right\rangle \right] + \lambda \left\langle \frac{f}{\sqrt{f^2 + \delta}}, g \right\rangle \\
&= \sum_{n=0}^{N-1} \left[\left\langle \left(I + \triangle t^n \triangle_{(u^n)}\right) p^{n+1} - p^n, z^n \right\rangle + \left\langle \triangle t^n p^{n+1}, g \right\rangle \right] + \lambda \left\langle \frac{f}{\sqrt{f^2 + \delta}}, g \right\rangle \\
&= \sum_{n=0}^{N-1} \left\langle \left(I + \triangle t^n \triangle_{(u^n)}\right) p^{n+1} - p^n, z^n \right\rangle + \left\langle \sum_{n=0}^{N-1} \triangle t^n p^{n+1} + \lambda \frac{f}{\sqrt{f^2 + \delta}}, g \right\rangle.
\end{aligned}$$

Thus, the adjoint system is approximated by

$$\begin{cases} p_i^N & = u_i^N \\ \frac{p_i^n - p_i^{n+1}}{\triangle t^n} & = \triangle_{(u^n)} p_i^{n+1}, \ n = N-1, \ldots, 0. \end{cases}, \ \forall v_i \in V \tag{4.3}$$

And, the descent direction of the control is given by

$$g_i = - \left(\sum_{n=0}^{N-1} \triangle t^n p_i^{n+1} + \lambda \frac{f_i}{\sqrt{f_i^2 + \delta}} \right), \ \forall v_i \in V. \tag{4.4}$$

The following lemma determines the stepsize Δt^n for the adjoint system (4.3).

Lemma 4.1. *The adjoint FE (4.3) is stable if*

$$\triangle t^n \leq \frac{2}{\lambda_{max}},$$

where λ_{max} is the largest eigenvalue of $-\triangle_{(u^n)}$.

Proof. Rewrite the adjoint system (4.3) as follows:

$$p^n = \left(I + \triangle t^n \triangle_{(u^n)}\right) p^{n+1}.$$

$$\begin{aligned} \| p^n \|_2 =& \| \left(I + \triangle t^n \triangle_{(u^n)}\right) p^{n+1} \|_2 \\ \leq& \| \left(I + \triangle t^n \triangle_{(u^n)}\right) \|_2 \| p^{n+1} \|_2 . \end{aligned}$$

Thus, the condition for stability is that

$$\| \left(I + \triangle t^n \triangle_{(u^n)}\right) \|_2 \leq 1.$$

Note that all eigenvalues of $-\triangle_{(u^n)}$ are nonnegative with

$$0 = \lambda_{min} < \lambda_i \leq \ldots \leq \lambda_{max}.$$

Hence,

$$\begin{aligned} \| \left(I + \triangle t^n \triangle_{(u^n)}\right) \|_2 \leq 1 &\iff 1 - \triangle t^n \lambda_{max} > -1 \\ &\iff \triangle t^n < \frac{2}{\lambda_{max}}. \end{aligned}$$

□

4.2. **Decision on stepsizes.** There are two stages of which stepsizes must be decided in optimal way: the Ricci flow (4.1) and the cost minimization (3.1). In this subsection, we present details on selecting step sizes based on the line search technique.

4.2.1. *Stepsize for the Ricci flow (4.1).* Note that the Lobachevski function (2.2) can be written as follow if the cone information f is considered :

$$\begin{aligned} E(u, f) := & \sum_{\triangle_{ijk} \in F} \left(\theta^i_{jk} \lambda_{jk} + \theta^j_{ki} \lambda_{ki} + \theta^k_{ij} \lambda_{ij} - \pi \left(u_i + u_j + u_k \right) \right) + \sum_{v_i \in V} \left(2\pi - f_i \right) u_i \\ & + 2 \sum_{\triangle_{ijk} \in F} \left(\Lambda \left(\theta^i_{jk} \right) + \Lambda \left(\theta^j_{ki} \right) + \Lambda \left(\theta^k_{ij} \right) \right) \end{aligned}$$

Then, we can easily check that

$$\nabla_u E(u, f) = K - f$$

and

$$\nabla^2_u E(u, f) = -\triangle_u \succeq 0.$$

Since the Ricci flow (4.1) is the negative gradient flow of the Lobachevski energy functional, we can take the step size $\triangle t^n$ as the largest $\triangle t$ which satisfies

$$E(u^n + \triangle t d^n, f) \leq E(u^n, f) - \sigma \triangle t (d^n)^T d^n, \tag{4.5}$$

where $d^n := -K^n + f$ and $\delta \in (0, 1)$.

4.2.2. *Stepsize for cost minimization (3.1).* As in 4.2.1, we can apply the line search technique for the minimization of the cost function $C_\delta[f]$. For the initial stepsize, we utilize the following Taylor series of $C_\delta[f + \epsilon g]$:

$$C_\delta[f + \epsilon g] \approx C_\delta[f] + \epsilon \nabla C_\delta[f]^T g + \frac{\epsilon^2}{2} g^T \nabla^2 C_\delta[f] g := \mathcal{Q}(\epsilon).$$

Note that $\mathcal{Q}(\epsilon)$ is the convex quadratic function in ϵ. Thus the optimal step size ϵ^* can be approximated by

$$\begin{aligned} \epsilon^* &= \underset{\epsilon>0}{\operatorname{argmin}} C_\delta[f + \epsilon g] \\ &\approx \underset{\epsilon>0}{\operatorname{argmin}} \mathcal{Q}(\epsilon) \\ \Longleftrightarrow \nabla \mathcal{Q}(\epsilon^*) &= 0 \\ \Longleftrightarrow \epsilon^* &= -\frac{\nabla C_\delta[f]^T g}{g^T \nabla^2 C_\delta[f] g} = \frac{g^T g}{g^T \nabla^2 C_\delta[f] g}. \end{aligned}$$

In this expression, the denominator $g^T \nabla^2 C_\delta[f]\, g$ can be computed by the following lemma.

Lemma 4.2.

$$\begin{aligned} g^T \nabla^2 C_\delta[f] g &= \frac{d^2}{d\epsilon^2} C_\delta[f + \epsilon g] \mid_{\epsilon=0} \\ &= \lambda \sum_{v_i \in V} \frac{\delta g_i^2}{\left(f_i^2 + \delta\right)^{\frac{3}{2}}} + \sum_{v_i \in V} \left\{ (z_i^N)^2 + u_i^N w_i^N \right\} \end{aligned}$$

where $w_i^n = \nabla z^n[f_i] \cdot g_i$.

Proof. Note that

$$C_\delta[f] = \lambda \sum_{v_i \in V} \sqrt{f_i^2 + \delta} + \frac{1}{2} \sum_{v_i \in V} \left(u_i^N\right)^2$$

and

$$\frac{d}{d\epsilon} C_\delta[f + \epsilon g] = \lambda \sum_{v_i \in V} \frac{(f_i + \epsilon g_i) g_i}{\sqrt{(f_i + \epsilon g_i)^2 + \delta}} + \sum_{v_i \in V} (u_\epsilon)_i^N (z_\epsilon)_i^N.$$

Let $w(t) := \nabla z[f] \cdot g$, $w(t)$ satisfies

$$\begin{cases} w'(t) & = \frac{d}{d\epsilon} \triangle_{u(t)} z_i[f+\epsilon g] \mid_{\epsilon=0} \\ & = \frac{1}{2} \sum_{\triangle_{ijk} \in F} \left[-\csc^2 \theta_{ij}^k \left(\frac{\partial \theta_{ij}^k}{\partial u_i} z_i + \frac{\partial \theta_{ij}^k}{\partial u_j} z_j + \frac{\partial \theta_{ij}^k}{\partial u_k} z_k \right) (z_j - z_i) \right. \\ & \qquad \left. -\csc^2 \theta_{ik}^j \left(\frac{\partial \theta_{ki}^j}{\partial u_i} z_i + \frac{\partial \theta_{ki}^j}{\partial u_j} z_j + \frac{\partial \theta_{ki}^j}{\partial u_k} z_k \right) (z_k - z_i) \right] \\ & \quad + \frac{1}{2} \sum_{j \sim i} \left(\cot \theta_{ij}^k (w_j - w_i) + \cot \theta_{ki}^j (w_k - w_i) \right) \\ & = \frac{1}{4} \sum_{\triangle_{ijk} \in F} \left[-\csc^2 \theta_{ij}^k \left(\cot \theta_{ki}^j (z_i - z_k) + \cot \theta_{jk}^i (z_j - z_k) \right) (z_j - z_i) \right. \\ & \qquad \left. -\csc^2 \theta_{ik}^j \left(\cot \theta_{ji}^k (z_i - z_j) + \cot \theta_{kj}^i (z_k - z_j) \right) (z_k - z_i) \right] \\ & \quad + \frac{1}{2} \sum_{j \sim i} \left(\cot \theta_{ij}^k (w_j - w_i) + \cot \theta_{ki}^j (w_k - w_i) \right) \\ w(0) & = 0. \end{cases}$$

Using $w(t)$, we can deduce that

$$\begin{aligned} \frac{d^2}{d\epsilon^2} C_\delta[f+\epsilon g] &= \lambda \sum_{v_i \in V} \frac{g_i \sqrt{(f_i+\epsilon g_i)^2+\delta} - (f_i+\epsilon g_i) \frac{(f_i+\epsilon g_i) g_i}{\sqrt{(f_i+\epsilon g_i)^2+\delta}}}{(f_i+\epsilon g_i)^2+\delta} g_i. \\ &\quad + \sum_{v_i \in V} \left[\left\{ (z_\epsilon)_i^N \right\}^2 + (u_\epsilon)_i^N (w_\epsilon)_i^N \right] \\ &= \lambda \sum_{v_i \in V} \frac{\delta g_i^2}{((f_i+\epsilon g_i)^2+\delta)^{\frac{3}{2}}} + \sum_{v_i \in V} \left[\left\{ (z_\epsilon)_i^N \right\}^2 + (u_\epsilon)_i^N (w_\epsilon)_i^N \right]. \end{aligned}$$

Thus,

$$\begin{aligned} g^T \nabla^2 C_\delta[f] g &= \frac{d^2}{d\epsilon^2} C_\delta[f+\epsilon g] \mid_{\epsilon=0} \\ &= \lambda \sum_{v_i \in V} \frac{\delta g_i^2}{\left(f_i^2+\delta\right)^{\frac{3}{2}}} + \sum_{v_i \in V} \left\{ (z_i^N)^2 + u_i^N w_i^N \right\}. \end{aligned}$$

□

In summary, we present the entire algorithm for conformal flattening based on the optimal control in the following table.

Algorithm 1 Optimal control for cone singularity

Procedure :
1. Determine the step size dt^n based on (4.5).
2. Compute $\mathbf{x}^{n+1}$ by solving (4.1) 'forward' in time.
2. Compute $\mathbf{p}^{n+1}$ by solving (4.3) 'backward' in time.
3. Compute the direction based on (4.4).
4. Perform an Armijo line search :
:Find smallest $j \in \{0, 1, \ldots\}$ with

$$C_\delta[f + \epsilon_0 \rho^j g] \leq C_\delta[f] - \sigma \epsilon_0 \rho^j \parallel g \parallel_2^2$$

and set $\epsilon^k = \epsilon_0 \rho^j$.
5. Update the cone singularity

$$f \leftarrow f + \epsilon g.$$

6. Stop or go to step 1.

5. Experimental Results

In this section, we perform several numerical experiments to validate the optimality of the suggested method. Throughout this section, we denote our method as **OCCF**(Optimal Controlled Conformal Flattening). For the comparison purpose, we compare the results with the **CETM** and **MAD**, which were discussed in Section 3.

All examples in here are presented with the number of cones n, the total cone angle $\Phi = \Sigma_{i \in V} \mid \phi_i \mid$ and the L^2 area distortion $\mathcal{A}$. Here, we select v_i as a cone only if it affects on the flattening, i.e., $\mid \phi_i \mid > 10^{-5}$. Since **MAD** utilizes the Yamabe equation to obtain cones, we solve the Ricci flow for final 2D embedding.

Initial triangulated meshes are pre-processed using the technique so called "Edge flipping [15]" to remove near flat triangles. Note that we didn't apply any post-processing for cones since the aim of this research is to focus on the construction of an optimal strategy for cone selecting. All computations were implemented with C++, and conducted on a regular personal with 16.0GB memory and 3.6GHz quad-CPU.

5.1. **Optimal Cone Angles.** In this subsection, we chose two objects for comparison : one is the heart shape with 852 vertices and the kitten with 878 vertices. For each object, we present two results for **CETM** to verify the greedy property of the method, and present L^2 area distortions of before and after 2D embedding as $\mathcal{A}^{before}$, $\mathcal{A}^{after}$ for **MAD**, respectively.

Figure 2 and 3 show the results computed by **CETM**, **MAD**, and **OCCF**. We compare our method with **CETM** for parameters which give similar distortion and cone angle with **OCCF**. For **MAD**, the results for $\lambda = 0.1,\ 0.5$ are compared. The numerical results show that **OCCF** is an optimal strategy for the total cone angle Φ among three methods, but seems not for the number of cones and L^2 area distortion. For the greedy-type method, **CETM**, we can see that there is a tradeoff between the number of cones and L^2 area distortion. However, for similar L^2

area distortion, the corresponding total cone angle is larger than other methods. Also, **CETM** yields higher distortion than **OCCF** for similar total cone angles.

In the case of the results from **MAD**, it shows an optimal L^2 area distortion among three methods. The number of cones from **MAD** is fewer than ours, but most of cones are located in tiny clusters, which can be resolved by post-processing such as "Extracting cones" in [1].

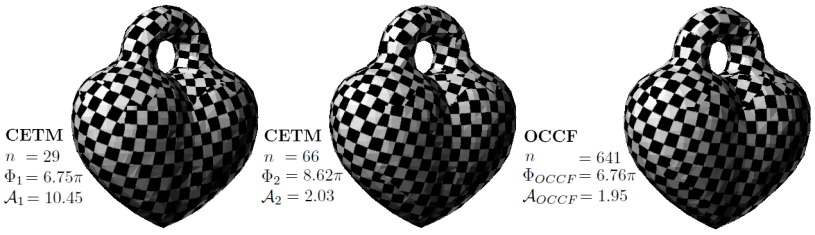

(a) Heart shape : **OCCF** ($\lambda = 0.5$), **CETM** ($\Phi_1 \backsimeq \Phi_{OCCF}$, $\mathcal{A}_2 \backsimeq \mathcal{A}_{OCCF}$)

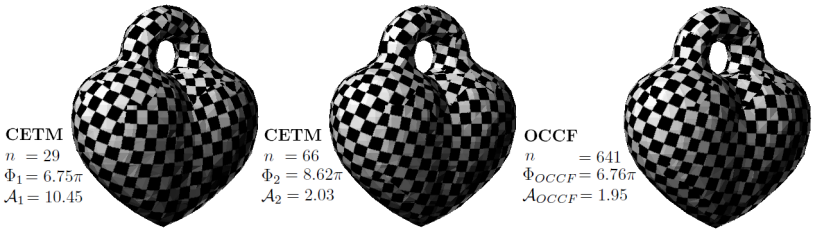

(b) Heart shape : **OCCF** ($\lambda = 0.1$), **CETM** ($\Phi_1 \backsimeq \Phi_{OCCF}$, $\mathcal{A}_2 \backsimeq \mathcal{A}_{OCCF}$)

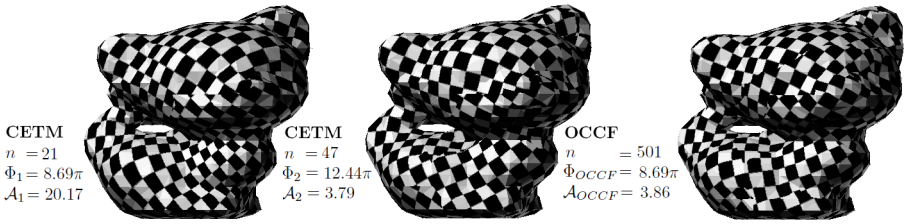

(c) Kitten : **OCCF** ($\lambda = 0.5$), **CETM** ($\Phi_1 \backsimeq \Phi_{OCCF}$, $\mathcal{A}_2 \backsimeq \mathcal{A}_{OCCF}$)

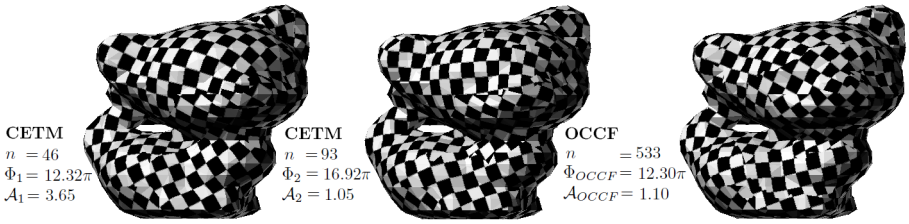

(d) Heart shape : **OCCF** ($\lambda = 0.1$), **CETM** ($\Phi_1 \backsimeq \Phi_{OCCF}$, $\mathcal{A}_2 \backsimeq \mathcal{A}_{OCCF}$)

FIGURE 2. Comparison with **CETM**. **OCCF** achieves the smalles total cone angle (right). **CETM** yields larger total cone angle for similar distortion (middle) and greater distortion for similar total cone angle (left).

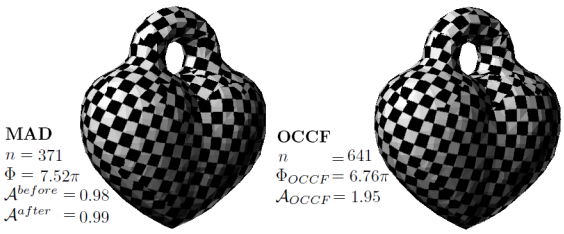

(a) Heart shape : **OCCF** ($\lambda = 0.5$), **MAD** ($\lambda = 0.5$)

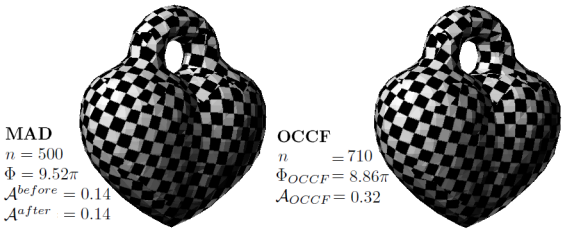

(b) Heart shape : **OCCF** ($\lambda = 0.1$), **MAD** ($\lambda = 0.1$)

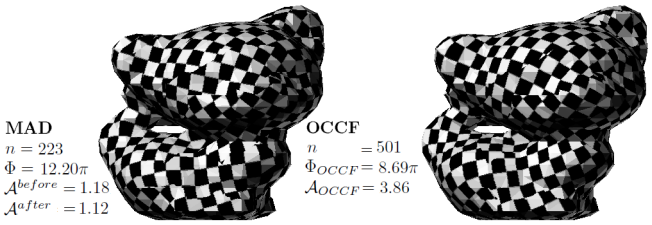

(c) Kitten : **OCCF** ($\lambda = 0.5$), **MAD** ($\lambda = 0.5$)

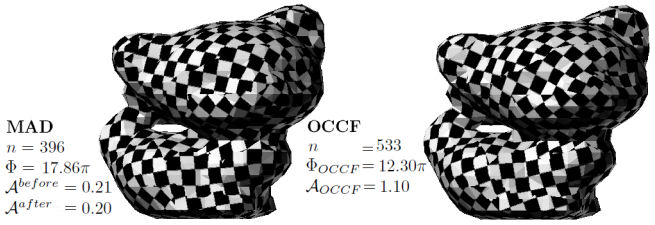

(d) Kitten : **OCCF** ($\lambda = 0.1$), **MAD** ($\lambda = 0.1$)

FIGURE 3. Comparison with **MAD**. **MAD** shows better area distortion (left), but it obtains larger total cone angle than **OCCF** (right).

5.2. **Optimality from the Ricci Flow.** In section 2, we verified that the solution u^{Yamabe} from the Yamabe equation is an approximated solution of u^* from the Ricci flow. We reveal that the approximation u^{Yamabe} can affect on the optimality of the given algorithm. Figure 4 shows the results computed by **MAD** (left) and **OCCF** (right) for the number six shape with 474 vertices. Although the geometry of this object is relatively simple, we can see that the L^2

area distortion of **MAD** gets larger after 2D embedding, which stems from the approximated solution u^{Yamabe}.

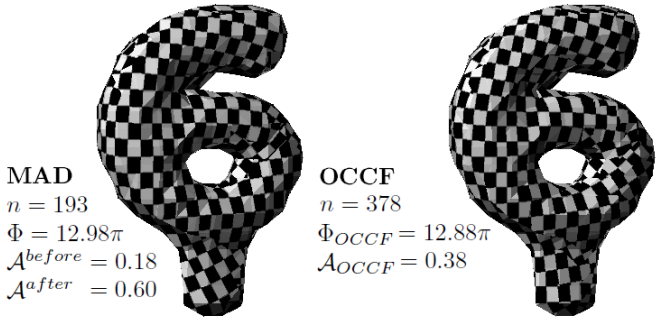

FIGURE 4. Optimal cone singularities of **MAD** (left) and **OCCF** (right) with $\lambda = 0.1$ for the number six shape. The approximated solution u^{Yamabe} yields the undesirable result that gets higher area distortion after the flattening. **OCCF** achieves smaller total cone angle and area distortion than **MAD**.

5.3. **The effect of tuning parameter λ.** The role of the parameter λ is to keep a balance between the L^2 area distortion and cone singularity. The effect of variation in λ is depicted in Fig 5, which visualizes the L^2 area distortion by colormap scaled from 0 (blue) to 0.25 (red). As we constructed, the parameter λ controls a tradeoff between the L^2 area distortion and cone singularity (total cone angle and the number of cones).

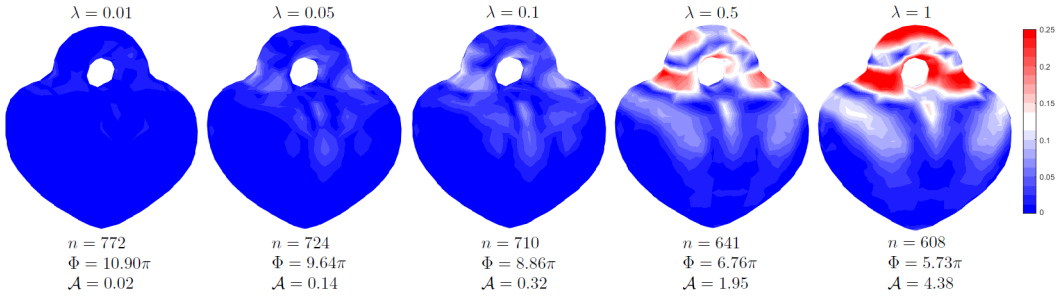

FIGURE 5. The larger λ, **OC** achieves larger area distortions and the smaller total cone angle. Although the number of cones becomes small, cones are placed over large regions.

6. CONCLUSION AND FUTURE WORK

We introduced a conformal flattening algorithm based on an optimal control for triangulated sufraces. We proposed the optimization problem for finding optimal cones utilizing the

Ricci flow rather than the Yamabe equation. The algorithm is presented with the mathematical background and numerical results show the optimality of the proposed method.

However, although our method is optimal in total cone angle, the L^2 area distortion seems to depend on the geometry of the object. Besides, proposed algorithm has a possible inefficiency issue generated by storing control squences. We postpone the resolution of above limitations in the near future.

ACKNOWLEDGMENTS

The research of Chohong Min and Yesom Park was supported by NRF grant 2017-006688, 2019R1A6A1A11051177. The research of Byungjoon Lee was supported by POSCO Science Fellowship of POSCO TJ Park Foundation and NRF grant 2017R1C1B1008626.

REFERENCES

[1] Yousuf Soliman, Dejan Slepčev, and Keenan Crane. Optimal cone singularities for conformal flattening. *ACM Transactions on Graphics (TOG)*, 37(4):105, 2018.

[2] Cindy Grimm and Denis Zorin. *Surface modeling and parameterization with manifolds: Siggraph 2006 course notes*. ACM, 2006.

[3] Rhaleb Zayer, Bruno Lévy, and Hans-Peter Seidel. Linear angle based parameterization. 2007.

[4] Zhengyu Su, Wei Zeng, Rui Shi, Yalin Wang, Jian Sun, and Xianfeng Gu. Area preserving brain mapping. In *Proceedings of the IEEE Conference on Computer Vision and Pattern Recognition*, pages 2235–2242, 2013.

[5] Bennett Chow and Feng Luo. Combinatorial ricci flows on surfaces. *Journal of Differential Geometry*, 63(1):97–129, 2003.

[6] Miao Jin, Junho Kim, Feng Luo, and Xianfeng Gu. Discrete surface ricci flow. *IEEE Transactions on Visualization and Computer Graphics*, 14(5):1030–1043, 2008.

[7] Liliya Kharevych, Boris Springborn, and Peter Schröder. Discrete conformal mappings via circle patterns. *ACM Transactions on Graphics (TOG)*, 25(2):412–438, 2006.

[8] Ashish Myles and Denis Zorin. Global parametrization by incremental flattening. *ACM Transactions on Graphics (TOG)*, 31(4):109, 2012.

[9] RS Hamilton. The ricci flow on surfaces. mathematics and general relativity, 237–262. *American Mathematical Society*, 1988.

[10] Boris Springborn, Peter Schröder, and Ulrich Pinkall. Conformal equivalence of triangle meshes. *ACM Transactions on Graphics (TOG)*, 27(3):77, 2008.

[11] Charles A Micchelli, Lixin Shen, Yuesheng Xu, and Xueying Zeng. Proximity algorithms for the l1/tv image denoising model. *Advances in Computational Mathematics*, 38(2):401–426, 2013.

[12] Emmanuel J Candes, Justin K Romberg, and Terence Tao. Stable signal recovery from incomplete and inaccurate measurements. *Communications on Pure and Applied Mathematics: A Journal Issued by the Courant Institute of Mathematical Sciences*, 59(8):1207–1223, 2006.

[13] Richard Baraniuk and Philippe Steeghs. Compressive radar imaging. In *2007 IEEE radar conference*, pages 128–133. IEEE, 2007.

[14] Yong-Liang Yang, Ren Guo, Feng Luo, Shi-Min Hu, and Xianfeng Gu. Generalized discrete ricci flow. In *Computer Graphics Forum*, volume 28, pages 2005–2014. Wiley Online Library, 2009.

[15] Feng Luo. Combinatorial yamabe flow on surfaces. *Communications in Contemporary Mathematics*, 6(05):765–780, 2004.